Magnetohydrodynamics, Vol. 30, No. 3, 1994

MHD CONTROL OF FREE CONVECTION IN HORIZONTAL BRIDGMAN CRYSTAL GROWTH

R. Moreau,[1] T. Alboussière,[2]
N. Ben-Salah,[1] J. P. Garandet,[2]
R. Bolcato,[1] and A. M. Bianchi[1]

The purpose of this paper is to present a summary of the results obtained on this subject in a joint-research program between MADYLAM and CEREM. After a few words on what is the actual problem and on the mathematical model, we present an asymptotic solution for large Hartmann numbers compared with numerical results for moderate Hartmann numbers. Finally, we show some of our first experimental results obtained with a mercury simulation that we call MASCOT. The initials MASCOT stand for MAgnetic Stabilization of COnvection and Turbulence.

A typical horizontal Bridgman crystal growth apparatus furnace includes a furnace, a water-cooled box, and, between them, an insulating part to adjust the axial temperature gradient. The semiconductor sample is molten at the hot side and withdrawn at the cold side in the solid state, hopefully as a single crystal. Because of the horizontal temperature gradient, there is always some natural convection, which is usually turbulent since the Grashoff number is of the order of 10^5. This convective flow is responsible for most of the defects of the crystal, such as segregation and striations (see, for instance, [1]). Then, a magnetic field is applied in order to reduce the fluid velocity and to stabilize all the disturbances.

Figure 1 shows the basis of our mathematical model. We consider a horizontal cylinder of given length L and width H. Its cross-sectional shape is determined by the equations $Z_1(Y)$ and $Z_2(Y)$ of the upper and lower parts of its contour. In the zero Prandtl number limit, the temperature gradient is uniform and given. We concentrate on the fully established regime outside the end regions where the fluid flow is not parallel to the axis. An important feature of this problem is the presence of buoyancy, which implies that, in the core, $\mathbf{j} \times \mathbf{B}$ is not curl-free, since it is not balanced only by the pressure gradient, as in pressure-driven flows. Here, the curl of $\mathbf{j} \times \mathbf{B}$ has to be balanced by the curl of buoyancy.

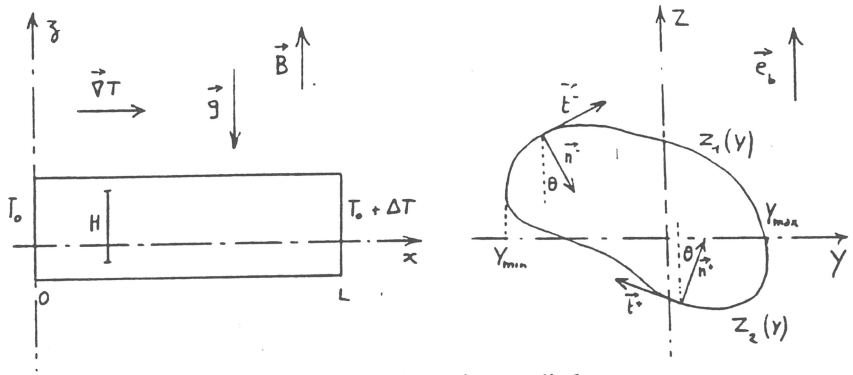

Fig. 1. Configuration studied.

[1]Laboratoire MADYLAM E.N.S.H.M.G. BP 95, F-38402 St. Martin d'Hères cedex, France.
[2]Commissariat à l'Energie Atomique, DTA/CEREM/DEM, Centre d'Etudes Nucléaires de Grenoble, 85 X, F-38041, Grenoble Cedex, France.

Published in Magnitnaya Gidrodinamika, No. 3, pp. 348-354, July-September, 1994.

0024-998X/94/3003-0282.$12.50

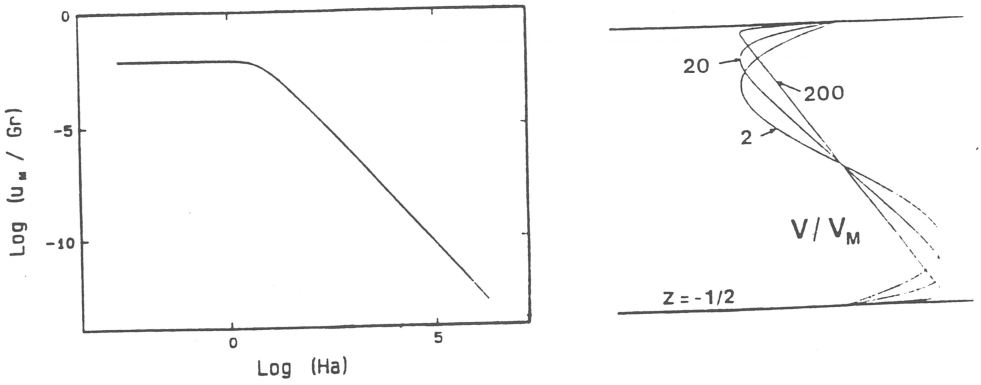

Fig. 2. 2D Exact solution for permanent flow.

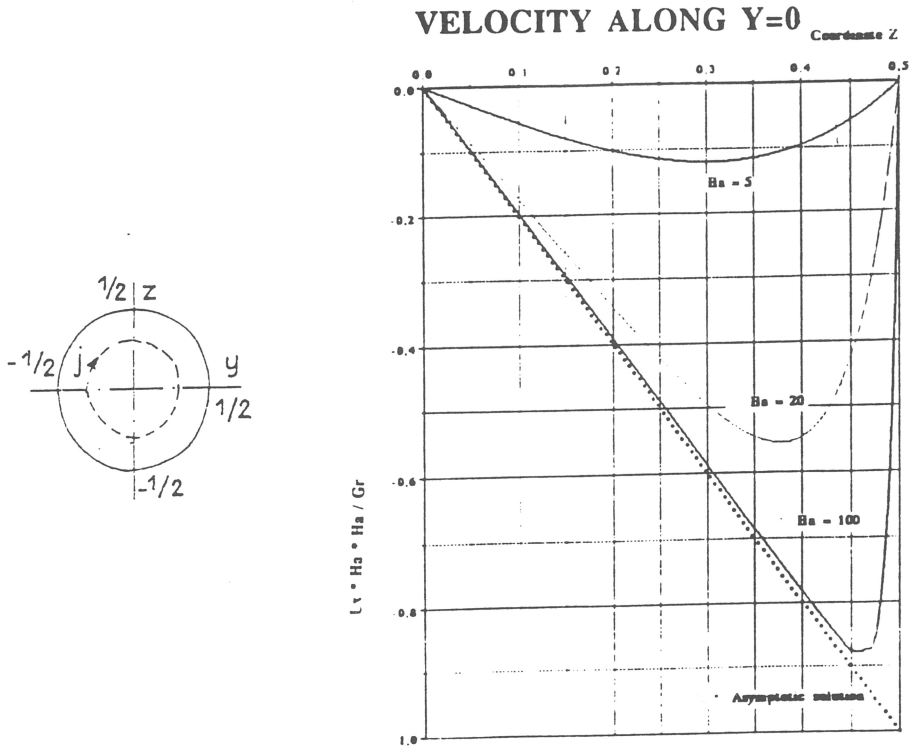

Fig. 3. Numerical solutions for Ha = 5, 20, 100 and asymptotic solution (circular insulating wall).

To solve the problem in the asymptotic limit Ha $\gg$ 1, we take once the curl of the Navier–Stokes equations, and twice the curl of Ohm's law. Then, instead of two equations for the well-known Elsasser variables U + B and U — B, we get two independent equations for variables M^+ and M^-, which are nothing but the curl of the Elsasser variables. The reader is refered to [2] and [3] for more details on this asymptotic analysis.

A numerical analysis is also carried out to gain some insight into the flow behavior in the moderate Ha number range (1 to 100). We investigate the solutions for several cross-sections: circles, square, 45 degrees inclined square (all of them are symmetric), and semicircle (nonsymmetric section). We use a finite element method paying special attention to the mesh-net; at least three meshes are located within the Hartmann layer. For all symmetric sections, the fluid goes through the negative X direction in the upper half of the section and closes in the positive X direction in the other half. We clearly show the damping effect of the Lorentz forces (Fig. 2), and this effect increases with the Hartmann number. When the walls are

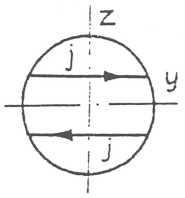

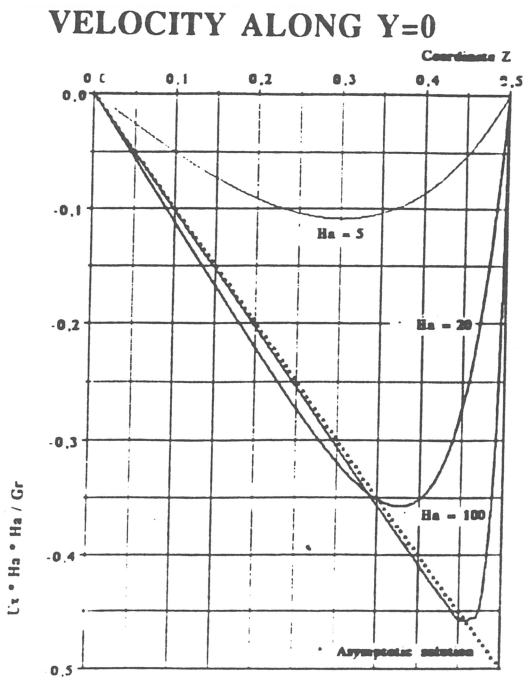

Fig. 4. Numerical solutions for Ha = 5, 20, 100 and asymptotic solution (circular conducting wall).

electrically perfectly insulating, the shear side layers for the square (Fig. 5) and the 45 degrees inclined square (Fig. 6) present a characteristic overvelocity. This overvelocity can be explained by the fact that in these regions, the electric current lines are parallel to the magnetic field **B** so that the Lorentz forces vanish.

For the insulating walls, the electric current lines close into the domain of the section and the boundary becomes an electric line (Fig. 3 and top of Figs. 5, 6, 7). When the walls are perfectly conducting, the electric current lines go normally through the walls and the boundary is isopotential (Fig. 4 and bottom of Figs. 5, 6, 7). In this case, we see that the overvelocities are much less than in the insulating walls case.

When the section is not symmetric (Fig. 7), the flow rearranges in three parts, one in the center through the positive X direction and the two others in the sides through the negative X direction.

The measurements performed with MASCOT concern the temperature distribution at the wall of a mercury cylinder. They are measured with 40 thermocouples; located at the wall, in contact with the mercury; 18 of them along a generatrix which is, until now, at 45° from the horizontal and give the axial temperature distribution on that generatrix; the others located on two circles, one in the middle of the cylinder, the other 1 cm from the cold end. Let us start with the temperature variation along the generatrix. At high magnetic field, we note a perfectly linear law (Fig. 8), which means that the convection has been almost completely damped out. The other curves demonstrate the influence of the remaining convection at moderate Hartmann numbers. It appears that, except within the two end regions, fully established flow exists, but with a temperature gradient G much smaller than $\Delta T/L$ as without convection. Now, at each end, there is a temperature jump, and, on that generatrix, the two jumps, ΔT_c and ΔT_H, are not symmetric.

Now, when we look at the temperature distribution on the middle circle, obviously located in the fully established regime, we observe, for all values of the magnetic field, a sinusoidal distribution, in very good agreement with the theoretical predictions. But, near the end, we notice not one but two maxima, and two minima as well (Fig. 9). The two maxima are located on both sides of 90°. These measurements demonstrate that the fluid flow in the two end regions is quite surprising. The streamlines do not remain within vertical planes, and the flow is three-dimensional. It is also clear that the typical length of the end region where the fluid flow is not fully established is much larger than $Ha^{-1/2}$. We think that some curious phenomena take place in these end regions.

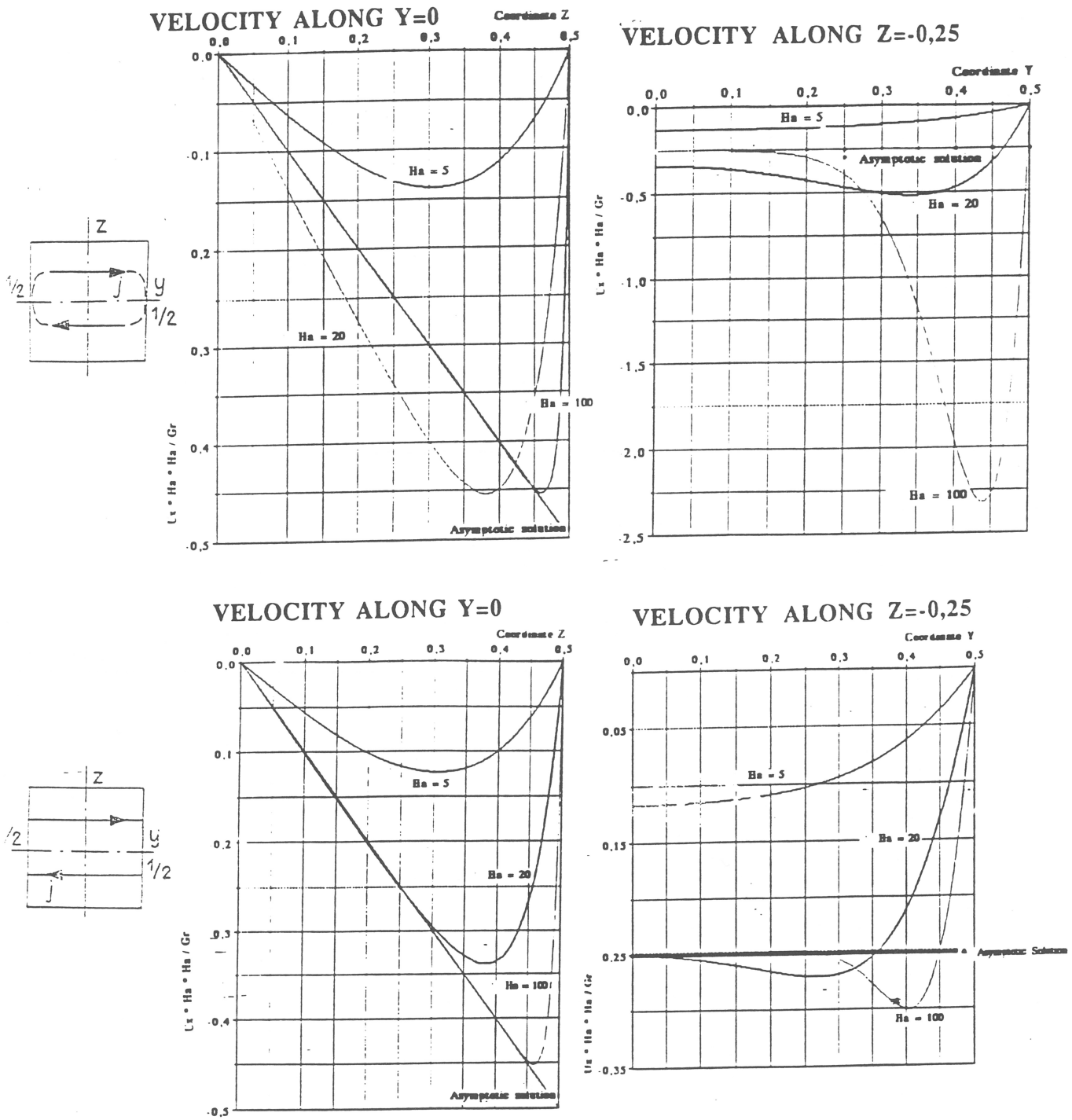

Fig. 5. Numerical solutions for Ha = 5, 20, 100 and asymptotic solution (square cross section). Above: insulating walls; below: conducting walls.

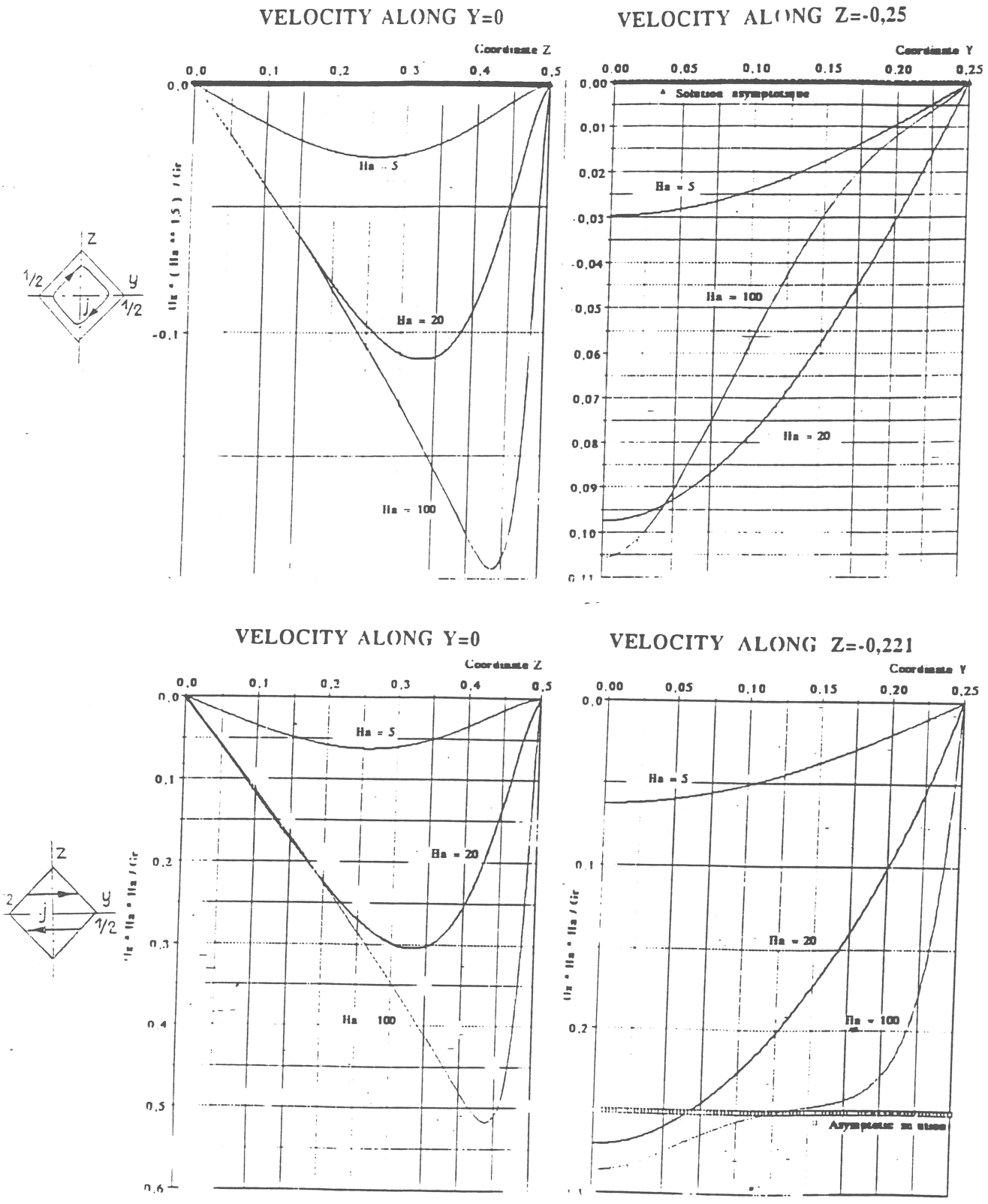

Fig. 6. Numerical solutions for Ha = 5, 20, 100 and asymptotic solution (45 degrees inclined square section). Above: insulating walls: below: conducting walls.

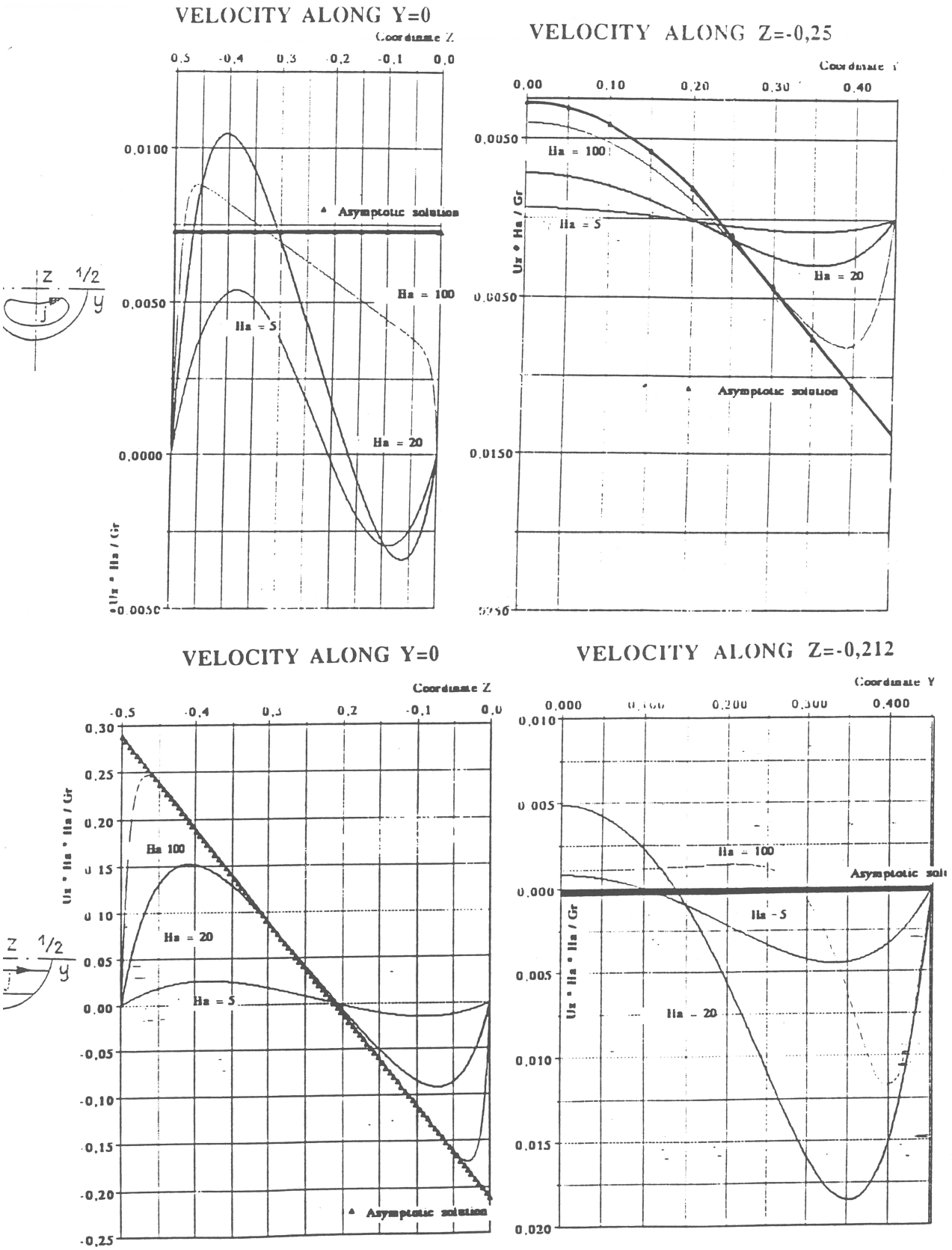

Fig. 7. Numerical solutions for Ha = 5, 20, 100 and asymptotic solution (semi-circular section). Above: insulating walls; below: conducting walls.

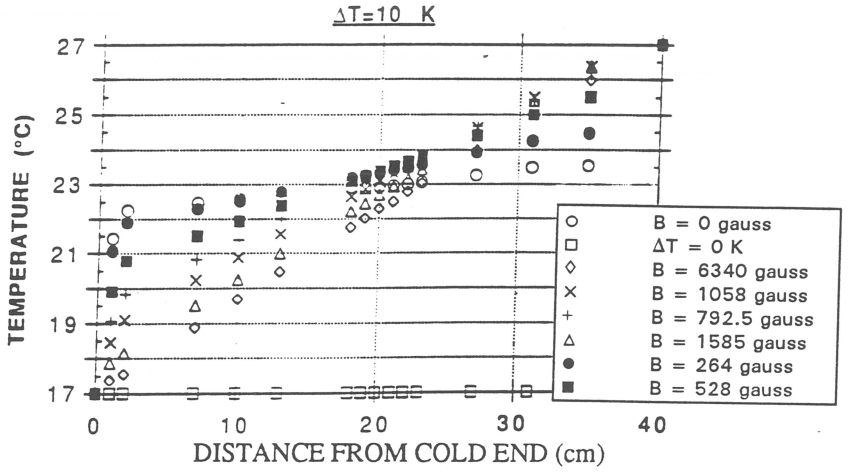

Fig. 8. Temperature distribution along a generatrix located at 45° above the horizontal diameter.

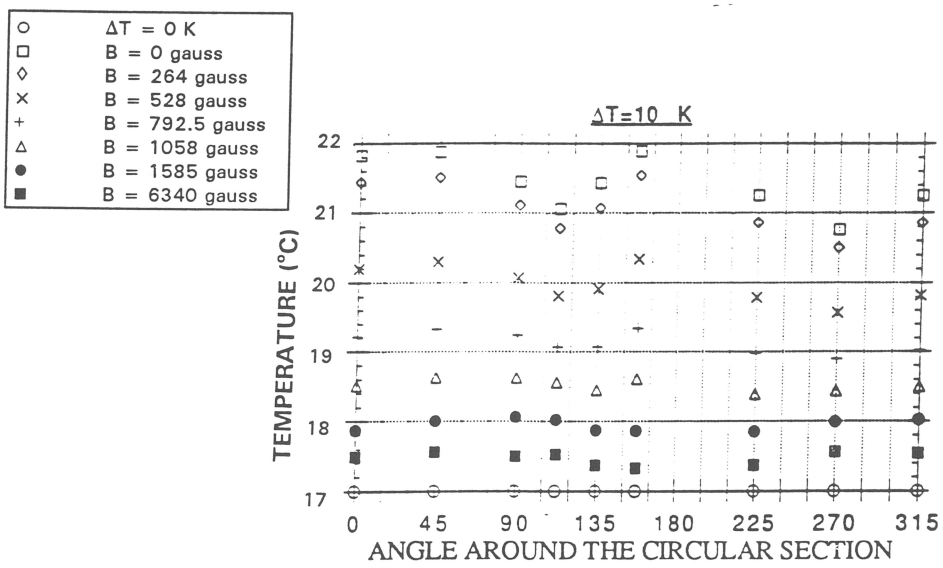

Fig. 9. Temperature distribution around a circle located near the cold end.

REFERENCES

1. W. E. Langlois, Annu. Rev. Fluid Mech., **17**, 191 (1985).
2. J. P. Garandet, T. Alboussière, and R. Moreau, Int. J. Heat Mass Transfer, **35**, 7410 (1992).
3. T. Alboussière, J. P. Garandet, and R. Moreau, J. Fluid Mech., **253**, 545 (1993).